The Abdus Salam International Centre for Theoretical Physics

United Nations Educational, Scientific and Cultural Organization

IAEA International Atomic Energy Agency

1856-30

2007 Summer College on Plasma Physics

30 July - 24 August, 2007

The particle-in-cell simulation method: Concept and limitations

M. E. Dieckmann

Institut fuer Theoretische Physik IV,
Ruhr-Universitaet,
Bochum, Germany

The particle-in-cell simulation method: Concept and limitations

Mark Eric Dieckmann

Institut für Theoretische Physik IV
Ruhr-Universität Bochum
D-44780 Bochum

Institutionen för teknik och naturvetenskap (ITN)
Linköpings universitet
Campus Norrköping
SE-60174 Norrköping

Book: C K Birdsall & A B Langdon, Plasma Physics Via Computer Simulation, Taylor & Francis Ltd (October 2004)

Contents

Why (and when) particle-in-cell (PIC) simulations?

- Particle-in-cell / Vlasov codes can address all collisionless plasma processes
- Such codes can be used to verify linearized plasma dispersion relations
- The plasma dynamics can be followed through its non-linear phase
- PIC simulations have an 'unlimited' dynamical range for the particle velocities and no boundary conditions along $\mathbf{v}$
- PIC codes have a limited signal-to-noise ratio and phase space density resolution
- PIC schemes parallelize well

What do PIC / Vlasov codes solve?

$$\nabla \times \mathbf{E} = -\frac{\partial \mathbf{B}}{\partial t} \tag{1}$$

$$\nabla \times \mathbf{B} = \mu_0 \epsilon_0 \frac{\partial \mathbf{E}}{\partial t} + \mu_0 \mathbf{J} \tag{2}$$

$$\nabla \cdot \mathbf{B} = 0 \tag{3}$$

$$\nabla \cdot \mathbf{E} = \rho / \epsilon_0 \tag{4}$$

Vlasov equation for phase space distribution $f(\mathbf{x}, \mathbf{v}, t)$

$$\frac{\partial f}{\partial t} + \mathbf{v} \cdot \nabla_x f + \frac{q}{m} (\mathbf{E} + \mathbf{v} \times \mathbf{B}) \cdot \nabla_v f = 0 \tag{5}$$

$$\rho(\mathbf{x}, t) = q \int_{-\infty}^{\infty} f(\mathbf{x}, \mathbf{v}, t)\, d\mathbf{v}, \;\; \mathbf{J}(\mathbf{x}, \mathbf{v}, t) = q \int_{-\infty}^{\infty} \mathbf{v} f(\mathbf{x}, \mathbf{v}, t)\, d\mathbf{v} \tag{6}$$

Numerics / Principle

Field equations

Replace continuous fields $\mathbf{B}(\mathbf{x},t)$, $\mathbf{E}(\mathbf{x},t)$ and Maxwell's equations by their discretized counterparts.

(1) Introduce finite spatial resolution $x \rightarrow j\Delta_x$ and finite time resolution $t \rightarrow j\Delta_t$, with integer values j.

(2) Replace differential operators by difference operators.
Example: $\frac{d}{dx}f(x) \rightarrow (f[(j+1)\Delta_x] - f[j\Delta_x])/\Delta_x$.

$\Rightarrow$ Replaces differential equations by algebraic equations.

Particle equations (PIC codes only)

Replace continuous probability distribution by phase space elements

$$f(\mathbf{x},\mathbf{v},t) \Rightarrow \sum_{i=1}^{N} S(\mathbf{x}-\mathbf{x}_i)\delta(\mathbf{v}-\mathbf{v_i}), \qquad (7)$$

where $S(\mathbf{x})$ is a shape function, e.g. a triangle.

$\Rightarrow$ Replaces phase space probability function by 'computational particles'.

Phase space distribution: Maxwellian distributions are often used.

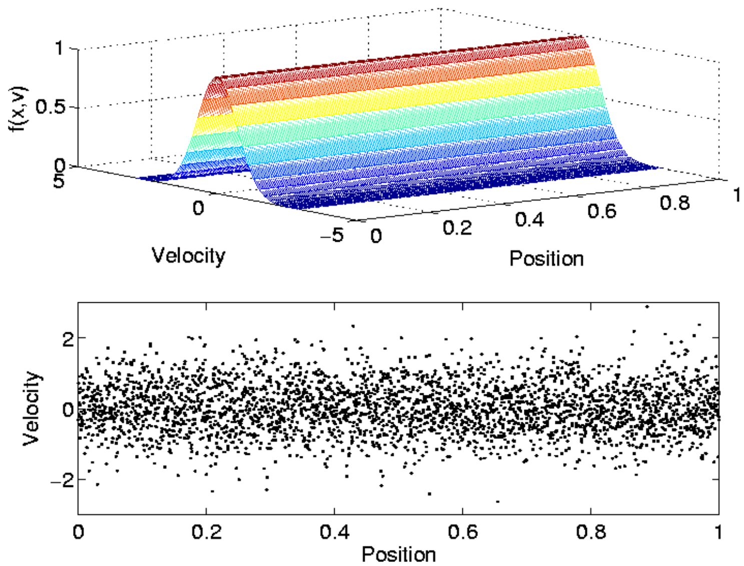

Quantitatively different results are sometimes obtained with Vlasov codes (upper phase space distribution) and PIC codes (lower phase space distribution)!

- If particle weights are equal, the statistical representation of the plasma close to the mean speed of the species is good.
- The statistical representation is poor, if $|v - \bar{v}| \geq 2v_t$ for a Maxwellian $\exp\left(-(v-\bar{v})^2 / 2\, v_t^2\right)$.

Particle-grid interaction

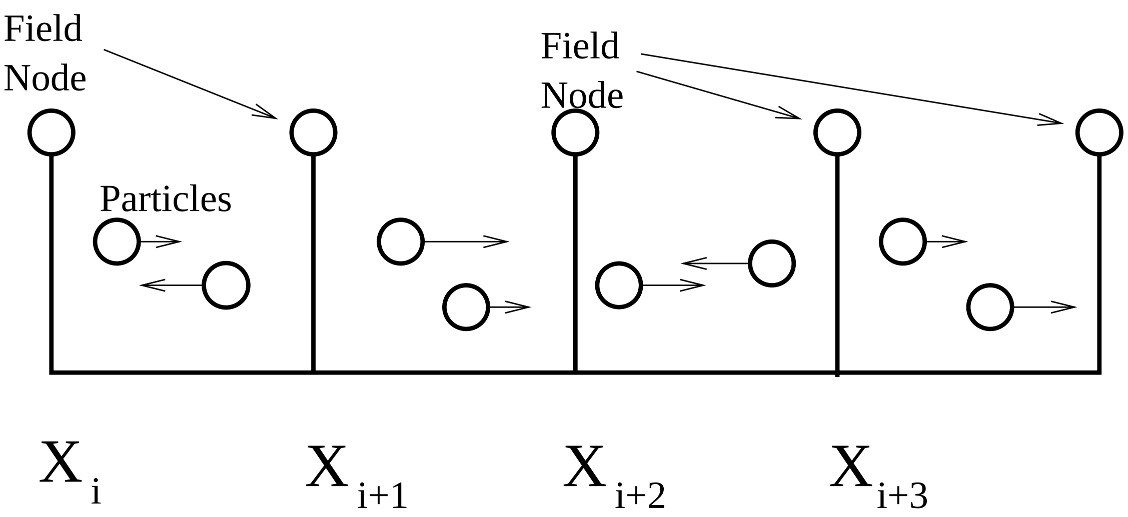

- The fields are defined on a grid (Field nodes).
- The particles move on 'continuous' paths.
- Particles interact with the grid through ρ and $\mathbf{J}$.
- The grid interacts with the particles through $\mathbf{E}$ and $\mathbf{B}$.

$\Rightarrow$ Interpolation schemes must be specified

- A computational electron is located between the cells $i, i+1$ with the positions X_i and X_{i+1}.
- It has the distance $D1$ from X_i and $D2$ from X_{i+1}.
- Electron charge Q is assigned to the grid nodes $i, i+1$: $C_i = f_1(D1, D2)$ and $C_{i+1} = f_2(D1, D2)$.
- Example: $C_i = Q\, D2$ and $C_{i+1} = Q\, D1 \quad$ if $(X_{i+1} - X_i) = 1$.

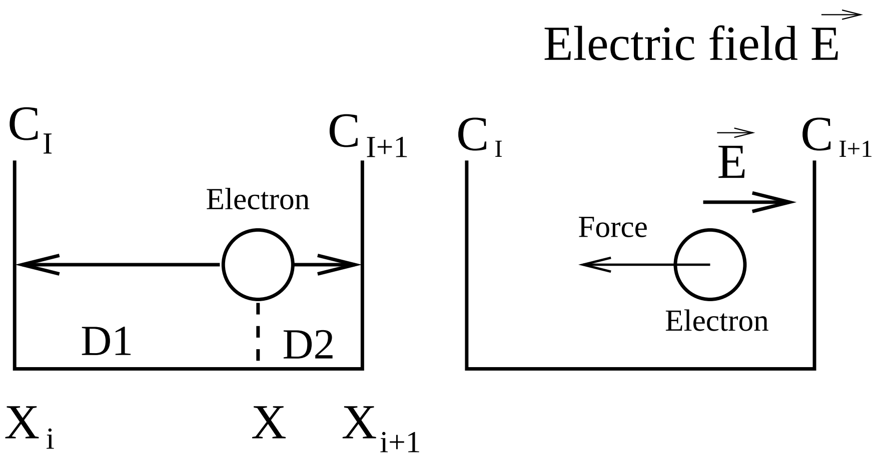

- Calculate potential Φ with $\nabla^2\Phi = -\rho/\epsilon_0$ with $\rho_i \sim C_i$ and $\rho_{i+1} \sim C_{i+1}$.
- $\mathbf{E} = -\nabla\Phi$.
- Interpolate $\mathbf{E}$ to particle position: $\mathbf{E}(x) = D2 \cdot \mathbf{E}(x_i) + D1 \cdot \mathbf{E}(x_{i+1})$

1. Initialize plasma phase space distribution:

– Place particles in space according to density

– Initialize velocities with random numbers

2. Initialize E and B fields

3. From E,B fields calculate acceleration

4. Multiply acceleration with time step

–> Velocity increment

5. Multiply velocity with time step

–> Position increment

6. From new positions and velocities:

Calculate new E,B

Limitations:

Known limitations with known consequence: Field discretization

- Spatial step $\Delta_x \approx$ Debye length $\lambda_d = v_t/\omega_p$.
- Numerical stability $\rightarrow$ small time step Δ_t.
  For my code: $\Delta_t = N_c \Delta_x / \sqrt{2}\, c$ with $0 < N_c < 1$.
- We have $\Delta_x = v_t/\omega_p$ and for $N_c = 1$ we get $\sqrt{2}\Delta_t \omega_p = v_t/c$.
  $\Rightarrow$ Low v_t requires high sampling rate. Critical speed $v_t \approx 10^6 m/s$.

Known limitations with unknown consequence:

Particle per cell count rates follow Poisson statistics $\rightarrow$ For N_e particles per cell, the relative fluctuations are $1/\sqrt{N_e}$.

- Fluctuations result in particle-wave collisions.
- Parametric instabilities speed up.
- Dispersive properties change. Bernstein modes are damped 'close' to $n\omega_c$.
- Signal-to-noise ratio is low.

Spatial grid effects

In 'continuous infinite plasmas': Fourier integral

Infinitely extended and continuous position x and wavenumber k domains.

$$f(x) \Leftrightarrow g(k) \tag{8}$$

$$f(x) = \int_{-\infty}^{\infty} g(k)\, \exp(\imath k x)\, dk \tag{9}$$

$$g(k) = \frac{1}{2\pi} \int_{-\infty}^{\infty} f(x)\, \exp(-\imath k x)\, dx \tag{10}$$

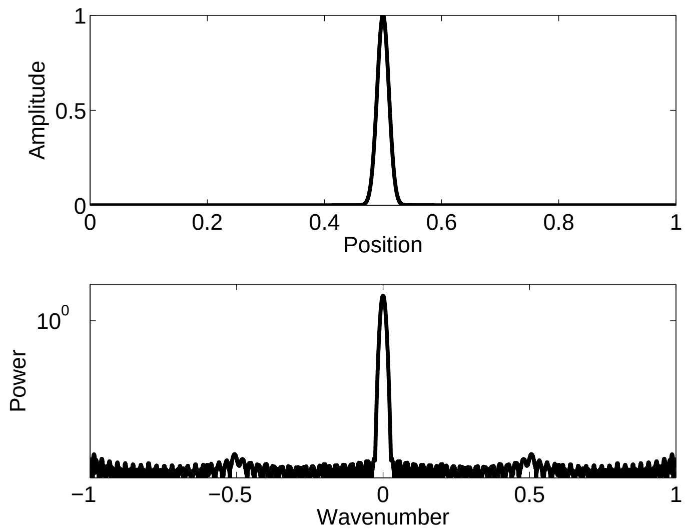

In 'continuous confined plasmas': Fourier series

Limited position $0 < x < L$, $f(x)$ continuous. Unlimited, discrete k spectrum.

$$f(x) \Leftrightarrow g_k = g(k_k) \tag{11}$$

$$f(x) = \sum_{k=-\infty}^{\infty} g_k \exp\left(\imath\, k_k\, x\right) \tag{12}$$

$$g_k = \frac{1}{L}\int_{x=0}^{x=L} f(x) \exp\left(-\imath\, k_k\, x\right) dx \tag{13}$$

Periodicity of $\exp(\imath\, k_i\, x)$ → The $f(x)$ is periodic, but not g_i.

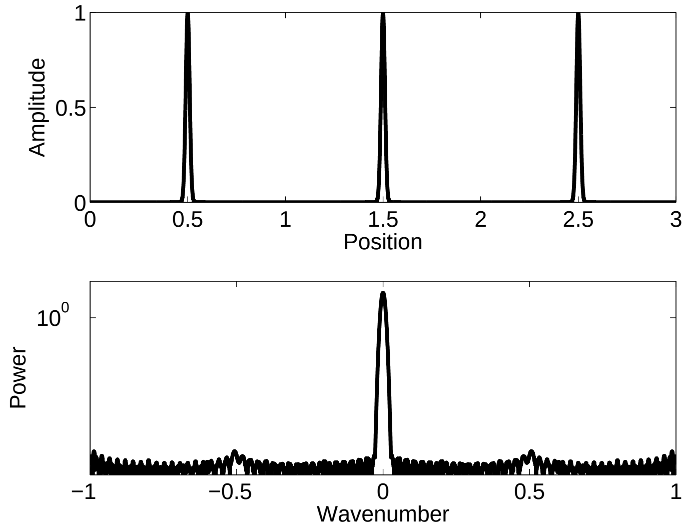

In 'PIC plasmas': Discrete Fourier transform

The PIC code cannot represent a Fourier series → The k-spectrum is truncated.

$$f_n = f(x_n) \Leftrightarrow g_k = g(k_k) \tag{14}$$

$$f_n = \sum_{k=0}^{N-1} g_k \exp\left(2\pi \imath kn/N\right), \; n = 0, ..., N-1 \tag{15}$$

$$g_k = \frac{1}{N} \sum_{n=0}^{N-1} f_n \exp\left(-2\pi \imath kn/N\right), \; k = 0, ..., N-1 \tag{16}$$

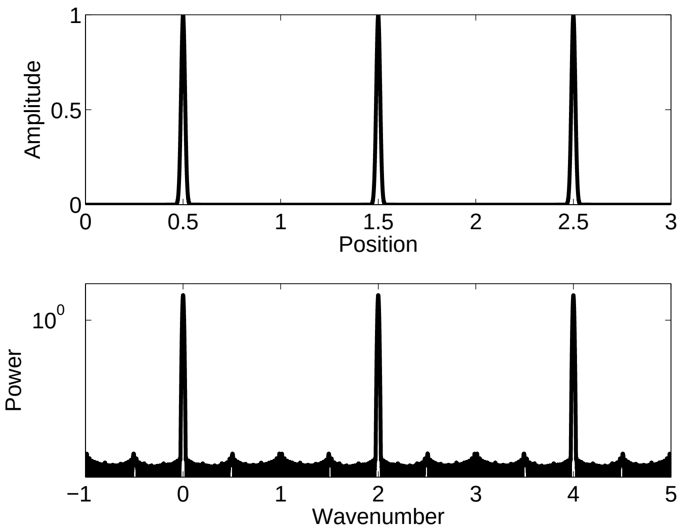

Finite grid instability

- Phase space distribution has rapid oscillations: $F(k_s, x) = \sin(k_s x)$.
- Grid imposes a maximum $k_{Ny} = \pi / \Delta_x$.
- A box with length L has the minimum $k_M = 2\pi / L$.

(a) $k_1 = k_{Ny}/25$ and $k_2 = k_{Ny}/100$. Integer values for k_1/k_M and k_2/k_M.

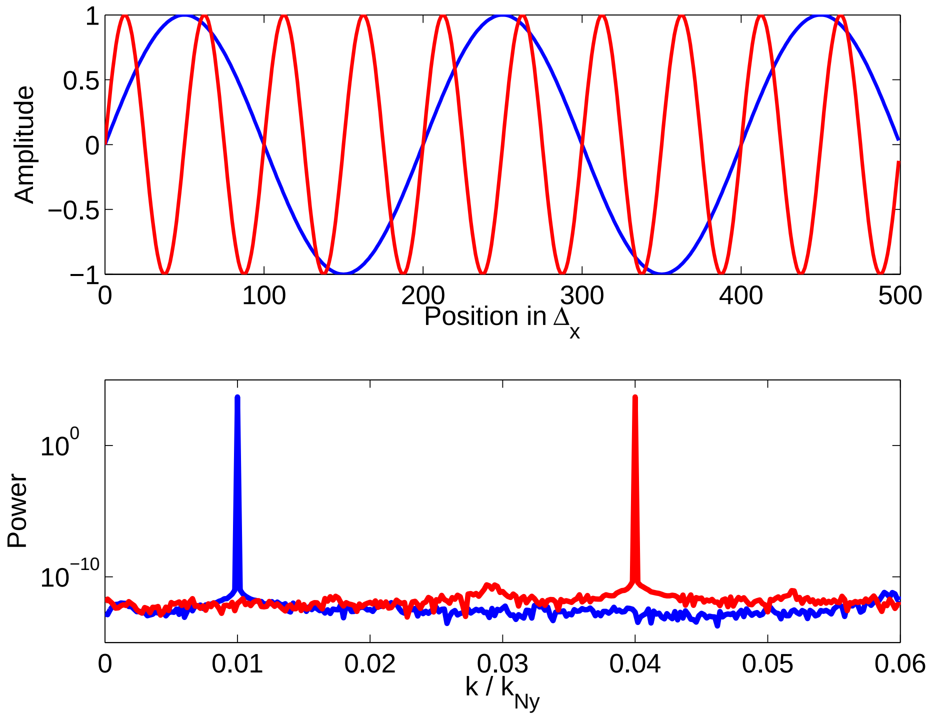

(b) $k_1 = k_{Ny}/25.25$ and $k_2 = k_{Ny}/100.25$. Non-integer k_1/k_M and k_2/k_M.

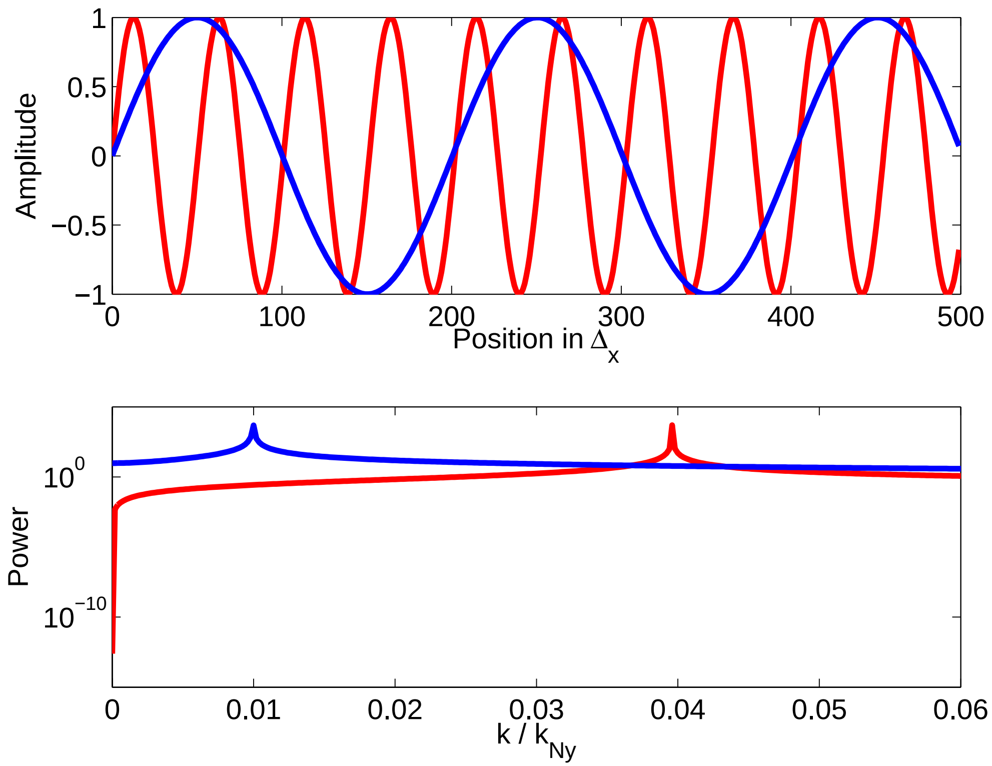

Wave oscillation is well-resolved.

Finite-box effects 'fill up' the k-spectrum: power leaks to other k (aliasing).

(c) $k_1 = k_{Ny}/2$ and $k_2 = 3\,k_{Ny}/2$. Integer values for k_1/k_M and k_2/k_M.

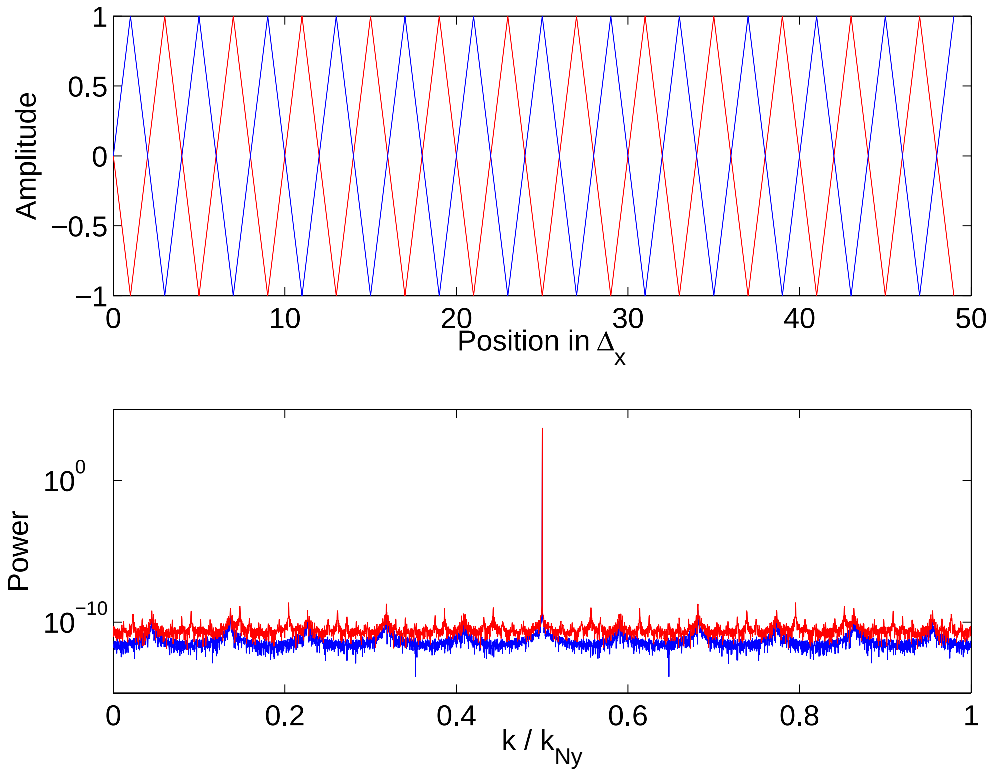

Peaks are identical in power but have different phases.

Some consequences:

- The aliasing is introduced by mapping oscillations with an 'unlimited' $k-$spectrum onto a grid with $|k| < k_{Ny}$.
- Case (3) showed that k_1, k_2 with $k_1 - k_2 = k_{Ny}$ differ only in phase.
- Truncated Fourier series → forced periodicity in x and k.

  Signals with k_1 and k_2 differing by $2\,k_{Ny}$ can't be distinguished!
- Relation to crystals / metals: *Brillouin zones*
- First Brillouin zone $|k\Delta_x| < \pi$. Other zones differ by $2\,k_{Ny} = k_g = 2\pi/\Delta_x$.
- In PIC simulations, elementary sine waves are actually not (!) eigenfunctions of the system.

Finite grid instability

Counterstreaming two-stream instability

$$1 - \frac{\omega_p^2}{\omega^2} = \frac{\Omega_b^2}{(\omega - kv_b)^2} + \frac{\Omega_b^2}{(\omega + kv_b)^2} \tag{17}$$

- Physical resonance term: $\omega - kv_b = 0$
- Aliasing: $\omega - (k + pk_g)v_b = 0$, with integer p.
- The term $k_g v_b$ has the dimension of a frequency. It is the grid crossing frequency ω_g of the particle beam.
- The beam drives many resonances $\frac{(\omega - p\,\omega_g)}{k} = v_b$. Only $p = 0$ is physical.
- Consequence: In non-relativistic 1D simulations with $\mathbf{k} \parallel \mathbf{v}_b$ the nonphysical instabilities are electrostatic and only heat the beam → Harmless.

Finite grid instability of relativistic beams in 2D

- The phase speeds of the waves are $\frac{\omega}{k} = v_b + p\,\frac{\omega_g}{k}$.
- For speeds $1 - \epsilon < v_b/c < 1$ and $\epsilon \ll 1$, a $p \neq 0$ introduces superluminal waves that couple directly to the beam. The resonance is sharp.
- Particle oscillations due to a wave with $\mathbf{k} \parallel \mathbf{v}_b$ couple through γ to other velocity components.

  Quiver motion acts as antenna!
- In 2D/3D simulations, obliquely propagating electromagnetic waves couple to the fast moving charge density modulation

  $\Rightarrow$ Electromagnetic radiation similar to free electron laser.

PIC simulation

- Spatially homogeneous system in x-y plane, periodic boundary conditions.
- Initially, $\mathbf{E} = 0$ and $\mathbf{B} = (0, 0, B_0)$ with $eB_0/m_e = \Omega_p/10$ (Ω_p = plasma frequency).
- Bulk electrons and protons at rest, number densities n_e and n_p.
- Counter-streaming proton beams with velocity vector $\pm(v_b, 0, 0)$ and $v_b = 0.8\,c$. Beam density: n_b each. Both beams differ in their temperature.
- $n_e = n_p + 2\,n_b$.
- Rectangular simulation box, sidelength $= 6\,\pi\,v_b\,/\,\Omega_p$. Resolved by a 1200×1200 mesh.
- The system is advanced in time for $t\Omega_p = 194$.

Results 1:

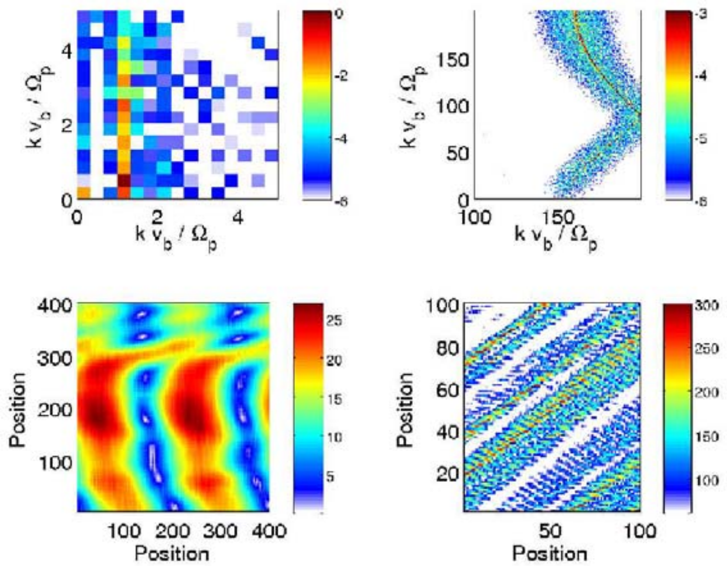

- Left plot, upper row: 10-logarithmic wavenumber (power) spectrum of physical wave. $\mathbf{v}_b$ is parallel to the x-axis.
- Right plot, upper row: 10-logarithmic wavenumber (power) spectrum of grid instability waves.
- Left plot, lower row: Low-pass filtered $|E_x + \imath E_y|$ in a rectangular sub-interval with the side length $2\,\pi\, v_b/\Omega_p$.
- Right plot, lower row: $|E_x + \imath E_y|$ in a rectangular sub-interval with the side length $\pi\, v_b\,/\,2\,\Omega_p$.

Results 2:

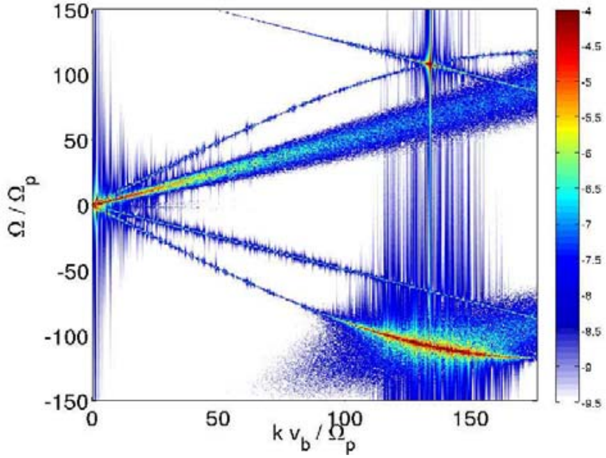

- Two straight lines going through $k = 0$, $\Omega = 0$: Beam dispersion relation.
- Two curved lines going through $k = 0$, $\Omega = 0$ (on this scale): Light modes.
- Straight line at large Ω parallel to the lower beam dispersion relation: Sideband separated from beam mode by grid crossing frequency.

Discussion

- The particle-in-cell simulation method is currently the tool of choice for the investigation of non-linear processes in kinetic, collision-less plasma.
- In contrast to fluid / magnetohydrodynamic codes, its resolution is set by the plasma Debye length → it can not be scaled to fit best a problem.
- Its signal-to-noise ratio is limited by noise. Noise can introduce 'unknown' modifications.
- The statistically poor representation of plasma by PIC simulations can give different results compared to Vlasov simulations.

  Example: Electron phase space holes can be more stable in Vlasov simulations: Dieckmann, Eliasson, Stathopoulos, Ynnerman, Phys. Rev. Lett. 92, 065006 (2004)
- The finite grid instability turns out to be a severe simulation constraint for the investigation of relativistic plasma flows. It can be reduced only moderately by finer grids.

  Dieckmann, Frederiksen, Bret, Shukla, Phys. Plasmas 13, 113110 (2006).